Contrib Mineral Petrol (2003) 146: 382–396
DOI 10.1007/s00410-003-0506-6

ORIGINAL PAPER

S. Jung · K. Mezger

U-Pb garnet chronometry in high-grade rocks—case studies from the central Damara orogen (Namibia) and implications for the interpretation of Sm-Nd garnet ages and the role of high U-Th inclusions

Received: 20 February 2003 / Accepted: 9 July 2003 / Published online: 29 August 2003

Abstract Garnets from different migmatites and granites from the Damara orogen (Namibia) were dated with the U-Pb technique after bulk dissolution of the material. Measured $^{206}Pb/^{204}Pb$ ratios are highly variable and range from ca. 21 to 613. Variations in isotope ($^{208}Pb/^{204}Pb$, $^{206}Pb/^{204}Pb$) and trace element (Th/U, U/Nd, Sm/Nd) ratios of the different garnets show that some garnets contain significant amounts of monazite and zircon inclusions. Due to their very low $^{206}Pb/^{204}Pb$ ratios, garnets from pelitic migmatites from the Khan area yield Pb-Pb ages with large errors precluding a detailed evaluation. However, the $^{207}Pb/^{206}Pb$ ages (ca. 550–500 Ma) appear to be similar to or older than U-Pb monazite ages (530 ± 1–517 ± 1 Ma) and Sm-Nd garnet ages (523 ± 4–512 ± 3 Ma) from the same sample. It is reasonable to assume that the Pb-Pb garnet ages define growth ages because previous studies are consistent with a higher closure temperature for the U-Pb system in garnet relative to the U-Pb system in monazite and the Sm-Nd system in garnet. For igneous migmatites from Oetmoed, Pb-Pb garnet ages (483 ± 15–492 ± 16 Ma) and one Sm-Nd garnet whole rock age (487 ± 8 Ma) are similar whereas the monazite from the same sample is ca. 30–40 Ma older (528 ± 1 Ma). These monazite ages are, however, similar to monazite ages from nearby unmigmatized granite samples and constrain precisely the intrusion of the precursor granite in this area. Although there is a notable difference in closure temperature for the U-Pb and Sm-Nd system in garnet, the similarity of both ages indicate that both garnet ages record garnet growth in a migmatitic environment. Restitic garnet from an unmigmatized granite from Omaruru yields similar U-Pb (493 ± 30–506 ± 30 Ma) and Sm-Nd (493 ± 6–488 ± 7 Ma) garnet ages whereas the monazite from this rock is ca. 15–25 Ma older (516 ± 1–514 ± 1 Ma). Whereas the monazite ages define probably the peak of regional metamorphism in the source of the granite, the garnet ages may indicate the time of melt extraction. For igneous garnets from granites at Oetmoed, the similarity between Pb-Pb (483 ± 34–474 ± 17 Ma) and Sm-Nd (492 ± 5–484 ± 13 Ma) garnet ages is consistent with fast cooling rates of granitic dykes in the lower crust. Differences between garnet and monazite U-Pb ages can be explained by different reactions that produced these minerals at different times and by the empirical observation that monazite seems resistant to later thermal re-equilibration in the temperature range between 750 and 900 °C (e.g. Braun et al. 1998). For garnet analyses that have low $^{206}Pb/^{204}Pb$ ratios, the influence of high-μ inclusions is small. However, the relatively large errors preclude a detailed evaluation of the relationship between the different chronometers. For garnet with higher $^{206}Pb/^{204}Pb$ ratios, the overall similarity between the Pb-Pb and Sm-Nd garnet ages implies that the inclusions are not significantly older than the garnet and therefore do not induce a premetamorphic Pb signature upon the garnet. The results presented here show that garnet with low $^{238}U/^{204}Pb$ ratios together with Sm-Nd garnet data and U-Pb monazite ages from the same rock can be used to extract geologically meaningful ages that can help to better understand tectonometamorphic processes in high-grade terranes.

Editorial responsibility: J. Hoefs

S. Jung (✉)
Max-Planck-Institut für Chemie, Abt. Geochemie, 3060,
55020 Mainz, Germany
E-mail: jungs@staff.uni-marburg.de
Fax: +49-6421-2828919

Present Address: Institut für Mineralogie, Kristallographie und Petrologie, Philipps Universität Marburg,
Lahnberge/Hans-Meerwein-Straße,
35032 Marburg, Germany

K. Mezger
Institut für Mineralogie, Universität Münster, Corrensstr. 24,
48149 Münster, Germany

Introduction

The reconstruction of the pressure-temperature-time (P–T-t) evolution of crustal sections is fundamental to

understand tectonic processes such as crustal thickening and thinning. This task requires the combination of metamorphic petrology and geochronology of different mineral phases. However, at the high temperatures affecting lower crustal sections during an orogeny, important rock-forming minerals (e.g., feldspars, micas) show open system behavior for the commonly used Rb-Sr and Sm-Nd geochronometers. On the other hand, the U-Pb system in zircon often records growth events that are much older than the metamorphic event of interest. In order to decide whether a mineral age represents a cooling age or growth age, it is essential to use different chronometers combined with well-constrained pressure-temperature estimates. In amphibolite- to granulite-facies metamorphic terranes, both peraluminous melts produced during anatexis and their high-grade metamorphic source rocks often contain monazite and garnet. Both minerals are ideal chronometers, because they have high closure temperatures and can yield precise and concordant U-Pb ages (Mezger et al. 1989; Parrish 1990; Bingen and van Breemen 1998; Hawkins and Bowring 1997, 1999). Therefore, they are suitable for constraining the time and duration of regional metamorphic and magmatic episodes.

Despite these advantages, the relationship between metamorphic reactions and the growth of monazite is not well established, because monazite can grow in a variety of environments following multiple metamorphic reactions (Smith and Barreiro 1990; Kingsbury et al. 1993, Bingen et al. 1996; Lanzirotti and Hanson 1996; Hawkins and Bowring 1997, 1999; Foster et al. 2000). Furthermore, there is still some debate about the closure temperature of the U-Pb system in monazite. Numerous studies have shown that moderate-sized monazite (< 200 μm) that cooled at moderate rates (< 15 °C/Ma) has inferred closure temperatures in excess of 750 °C (Copeland et al. 1988; Parrish 1990; Hawkins and Bowring 1997; Bingen and van Breemen 1998; Braun et al. 1998; Möller et al. 2000; Jung and Mezger 2001). However, there is experimental and empirical evidence that monazite can lose Pb below 700 °C (Suzuki et al. 1994) suggesting that the U-Pb isotope system can be reset at upper amphibolite facies conditions. Some of the differences in the estimate of the closure temperature may be due to the problem that it is still not clear whether monazite loses Pb by diffusion or during recrystallisation of metamict material, as it is observed in zircons. Additionally, a variety of primary and secondary processes can influence the age and concordance of monazite including (1) growth of new monazite around pre-existing crystals (Copeland et al. 1988; Kingsbury et al. 1993), (2) episodic growth of monazite (Parrish 1990; Lanzirotti and Hanson 1995), (3) high-temperature Pb loss (Parrish and Tirull 1989), (4) U-Th disequilibrium, resulting in reverse discordance (Schärer 1984), (5) mineral-fluid interaction with dissolution-reprecitipation of monazite along the retrograde metamorphic path (DeWolf et al. 1993) and (6) recrystallisation of metamict monazite.

Garnet can provide essential information on the P–T path and also precise geochronological information on rates of metamorphic processes using the Sm-Nd, U-Pb and Rb-Sr systems (Christensen et al. 1989; Mezger et al. 1989; Vance and O'Nions 1990; Burton and O'Nions 1991; Mezger et al. 1992; Vance et al. 1998; Vance and Harris 1999; Foster et al. 2000; Jung and Mezger 2001). A closure temperature of > 800 °C has been proposed for the U-Pb system in garnet (Mezger et al. 1989) and consequently this system may be the most promising in determining mineral growth ages in high grade terranes. The Sm-Nd method is commonly used for garnet dating, because the garnet structure strongly discriminates Nd relative to Sm, resulting in high Sm/Nd ratios that are favorable for precise geochronology. However, estimates of the closure temperature of the Sm-Nd system in garnet have been strongly debated over the years and published values range from 900 to 500 °C (Humphries and Cliff 1982; Cohen et al. 1988; Jagoutz 1988, Hensen and Zhou 1995). Mezger et al. (1992) proposed a value of 600 ± 30 °C for slowly cooled rocks by comparing Sm-Nd whole rock-garnet ages with mineral ages using other isotopic systems from the same rocks and metamorphic terrane. However, the discussion on the closure temperature of Sm-Nd in garnet is extremely weak because it is obvious that not all temperatures that have been published are correct. A critical review of all the data indicates that in terranes with cooling rates of 1–5 °C/Ma the closure temperature is slightly lower than for the U-Pb system in titanite. There are higher estimates, but they have either no real constraint by a real temperature (Humphries and Cliff 1982; Cohen et al. 1988; Jagoutz 1988) or are from contact metamorphic rocks, where the thermal pulse is short and resetting requires higher temperatures (e.g. Henson and Zhou 1995). A lower value for the closure temperature of Sm-Nd relative to U-Pb has important consequences for the interpretation of P–T-t paths, since in this situation Sm-Nd garnet ages would not reflect the time of peak metamorphism, but probably some part of the retrograde path of metamorphism.

Uranium-Pb and Sm-Nd data of garnet are usually difficult to interpret in a geologic context due to low concentrations of U, Pb, Sm and Nd in garnet and the common observation that the trace element budget of the garnet may be controlled by tiny inclusions of zircon, monazite and allanite with high concentrations of these elements (Hensen and Zhou 1995; Zhou and Hensen 1995; DeWolf et al. 1996, Vance et al. 1998; Jung and Mezger 2001). Therefore, if inclusion-bearing garnets are dated, it must be assumed that the garnet grew simultaneously with the inclusions or that the inclusions were in isotopic equilibrium with the host garnet.

In this paper, U-Pb garnet ages are presented for migmatites and peraluminous granites from the central Damara orogen of Namibia. These ages are discussed together with published Sm-Nd garnet ages and U-Pb monazite ages from the same samples (Jung et al. 2001;

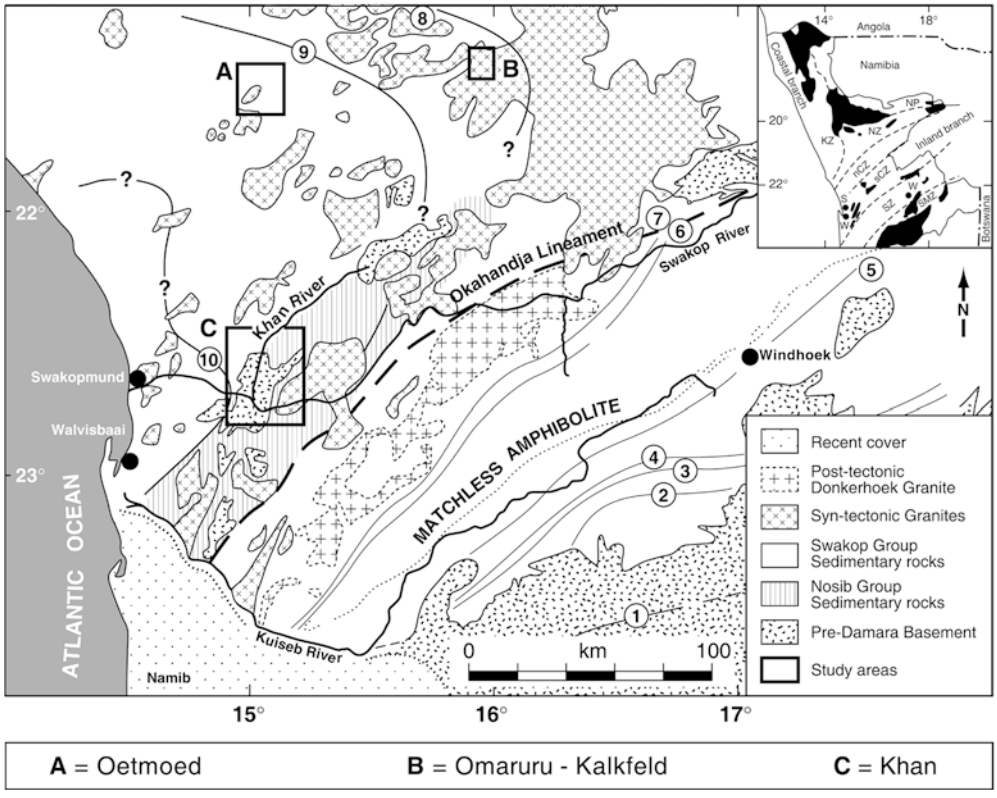

Fig. 1 Generalized geological map of the central Zone of the Damara orogen, Namibia with the position of the different localities mentioned in the text: *A* Oetmoed Granite–Migmatite Complex, *B* road-cut Omaruru-Kalkfeld, *C* Khan area. *Abbreviations* in *inset*: *KZ* Kaoko Zone, *NP* Northern Platform, *NZ* Northern Zone, *nCZ* northern Central Zone, *sCZ* southern Central Zone, *SZ* Southern Zone, *SMZ* Southern Margin Zone. *Isograd map* (Hartmann et al. 1983) gives the distribution of regional metamorphic isograds within the southern and central Damara orogen. Isograds: *1* biotite-in, *2* garnet-in, *3* staurolite-in, *4* kyanite-in, *5* cordierite-in, *6* andalusite <—> sillimanite, *7* sillimanite-in according to staurolite-breakdown, *8* partial melting due to: muscovite + plagioclase + quartz + H_2O <—> melt + sillimanite, *9* K-feldspar + cordierite-in, *10* partial melting due to: biotite + K-feldspar + plagioclase + quartz + cordierite <—> melt + garnet

Jung and Mezger 2003). It is shown that the Pb isotope data obtained on garnet with high $^{206}Pb/^{204}Pb$ and $^{208}Pb/^{204}Pb$ ratios may be influenced by inclusions of zircon and monazite, however, reliable ages can be derived from these garnets suggesting that the inclusions are not significantly older than the time of garnet growth.

Geologic setting

The Damara orogen exposes a deeply eroded section through a Pan African mobile belt that can be divided into a N-S trending coastal branch, the Kaoko belt, and a NE-SW trending intracontinental branch (see inset in Fig. 1). This mobile belt has been divided into several zones based mainly on stratigraphy, metamorphic grade, structure and geochronology. Granites with Rb-Sr whole rock ages between 650 and 460 Ma are the most common igneous rock type (ca. 96%) and the remaining intrusions are equally divided between gabbro/diorite and tonalite/granodiorite. Pre-Damara basement gneisses are overlain by Neoproterozoic to Paleozoic metasedimentary sequences comprising quartzose sandstones, mica schists, calc-silicate rocks, marble, banded iron-stones, Al-rich metapelites, migmatites, metacarbonates and conglomerates (for a review see Miller 1983). In the Central Zone (Fig. 1), the metamorphic grade increases from east to west reaching high-grade conditions with local partial melting in the coastal area (Hartmann et al. 1983). Recent P–T estimates indicate medium-pressure high-temperature granulite facies conditions with temperatures >700 °C at 4–6 kbar (Masberg et al. 1992; Jung et al. 1998a; 2000b; Jung and Mezger 2003). It is widely accepted that the depositional, metamorphic and deformational history of the central Damara orogen is complex (Miller 1983). The early history is characterized by deposition of a widespread flysch facies. This sequence was deposited in relatively deep water of the Khomas basin, at least in part on thin continental crust. The early crustal thinning took place around 700 Ma ago and may have been accompanied by limited seafloor spreading. The outcome of this limited seafloor spreading is probably the 300-km-long belt of the "Matchless Amphibolite" which has N-MORB to E-MORB affinities (Schmidt and Wedepohl 1983) and strikes parallel to the orogen. Throughout the central part of the orogen, this metasedimentary sequence was folded during one or more low to medium

P metamorphic episodes. The earliest deformational event is considered only slightly older than ca. 650 Ma because D_1 recumbent folds were intruded by ca. 650-Ma-old granitic rocks in the central zone (Miller 1983). However, in view of the recent geochronological data the radiometric ages of 650 Ma are considered to be of doubtful geologic significance because they are exclusively based on Rb-Sr whole rock analyses. No precise mineral ages are available for these rocks. Precise U-Pb radiometric ages are still scarce for Damaran syn-orogenic plutonic rocks. Some of the syenites in the central zone intruded close to the first peak of regional metamorphism probably around 540 Ma (Jung et al. 1998b). Precise U-Pb titanite ages for the volumetrically minor quartz diorites in the central zone are around 536 ± 6 Ma (Jung et al. 2003) and it seems very likely that these intrusive rocks are products of spatially limited mafic underplating. Deformation and plutonism related to D_2 must have occurred before ca. 540 Ma because at that time, D_3 doming produced not only spectacular domes consisting of pre-Damara basement and granite but was also accompanied by intrusion of voluminous granitic bodies. All monazite fractions from the metasedimentary rocks and migmatites from the Central Damara orogen are nearly concordant and define three different episodes, ca. 540 Ma, ca. 520–510 Ma and ca. 490–470 Ma (Jung et al. 2000b, Jung and Mezger 2001, 2003) Among the three age groups observed, the ca. 540 Ma age is interpreted to represent the age of M_1 whereas the ca. 520–510 Ma ages are closely related to the peak of regional metamorphism associated with M_2. The Sm-Nd garnet analyses, although less precise, support the proposition that peak metamorphism culminated in limited in-situ partial melting at 520–500 Ma. The third interval between ca. 490–470 Ma can be attributed to a third growth episode of monazite, associated with reheating of the crustal segment by voluminous intrusions of granite during M_3. This suggestion is confirmed by the U-Pb monazite and titanite ages obtained on the A-type granites (ca. 494–488 Ma; Jung et al. 2000a) and Sm-Nd whole rock-garnet ages obtained on magmatic garnets (ca. 492–484 Ma, Jung et al. 2001). The oldest monazite ages provide a reasonable estimate for the initiation of monazite growth on the prograde path prior to anatexis. The metamorphic grade of M_1 is unknown because there is no textural evidence for the nature of the monazite-producing reaction and little is known about the prograde paragenesis of monazite in metamorphic rocks. It is suggested that it probably must have exceeded 525 ± 25 °C at pressure of 3 ± 0.25 kbar which are considered to be the minimum conditions for the growth of metamorphic monazite in pelites (Smith and Barreiro 1990). The regional metamorphic assemblage cordierite-sillimanite-K-feldspar presumably developed afterwards during M_2 or M_3 and monazite probably continued to grow during prograde heating. In this case, a conservative estimate is that monazite is immune to isotopic re-equilibration at conditions up to those of the sillimanite-cordierite-K-feldspar zone. The M_3 ages range from 487 ± 1 Ma to 470 ± 1 Ma whereas the ages obtained from the post-collisional A-type granites and S-type granites range from ca. 494 to 488 Ma and from ca. 492 to 484 Ma, respectively. Therefore, multiple pulses of igneous intrusions could account for the range of metamorphic ages younger than 487 Ma seen in the gneisses and most of the crustal plutonism observed occurred later than 500 Ma in a setting probably characterized by extension and uplift. To the south-east, the Okahandja Lineament Zone separates the Central Zone from the Southern Zone. In the Southern Zone, regional metamorphism is characterized by a Barrovian-type sequence with a general increase in the metamorphic grade from south to north. The metamorphic conditions range from low to medium pressures and reached up to 8 kbar at maximum temperatures of ca. 600 °C.

Sample description of migmatites and granites

Metapelites and pelitic migmatites (Khan and Oetmoed areas)

Metasedimentary migmatites (samples K 4.7, K 4.1, K 4.2) from the Khan area (Fig. 1) consist of melanosomes containing biotite-plagioclase-quartz-K-feldspar-cordierite-garnet-sillimanite and leucosomes containing quartz-plagioclase-K-feldspar-biotite-garnet. Based on different initial ϵ Nd values between melanosomes and leucosomes (Jung et al. 2003), the latter are interpreted as melts injected into the metasedimentary rocks. The notable difference between non-migmatitic metasedimentary rocks (i.e., metapelite sample K 4.5) and migmatites is the larger amount of garnet in the migmatites. It is therefore suggested that in this case the garnet formed as a consequence of an incongruent dehydration-melting reaction involving biotite, sillimanite, quartz and probably cordierite. One migmatite sample from the Oetmoed migmatite complex (sample 89.19) is dominated by injected granite material. Biotite- and garnet-rich schlieren define a swirling foliation and are interpreted as the result of the disruption and redistribution of the pelitic material during intrusion of the granite.

Meta-igneous migmatite (Oetmoed area)

In the meta-igneous migmatite sample (sample 89.80) from the Oetmoed Migmatite Granite Complex (Fig. 1) the distinction between pre-existing igneous material and newly formed melt is less clear due to the felsic nature of the host rock. Rarely, mafic schlieren consisting exclusively of biotite also define a swirling foliation and are in this case interpreted as the result of the disruption and redistribution of the granitic material during remelting. Within the newly formed melt, garnet occurs as large grains that are up to 5 cm in diameter

with haloes consisting predominantly of quartz and minor amounts of plagioclase. Inclusions of quartz in garnet are common.

Granites (Khan and Oetmoed areas, road cut Omaruru-Kalkfeld)

In the medium-grained granites from the Khan area (samples 94.297, 94.298) garnet occurs as large crystals up to 2 cm in diameter. The garnets have embayed crystal faces, some crystals contain inclusions of sillimanite and quartz. Late-tectonic granites from the Oetmoed Migmatite Granite complex (samples 26.5, 89.52, 89.53) are medium to coarse-grained, white to light grey and homogeneous. Textures are mainly equigranular, but some samples have K-feldspar megacrysts up to 10 mm in length. These granites contain small, 1–5-mm large euhedral to subrounded, almandine- and spessartine-rich garnets with tiny inclusions of biotite and apatite needles (Jung et al. 2001). Late-tectonic restite-bearing granite from road cut Omaruru-Kalkfeld (samples S 84, S 85) is enriched in biotite and garnet relative to the late-tectonic granites from Oetmoed. Individual garnet grains are large (5–10 mm) and irregularly shaped with abundant inclusions of quartz.

Garnet compositions

Garnet is predominantly almandine-pyrope-spessartine solid solution with a minor grossular component. Most garnets from the metasedimentary rocks and migmatites of the Damara orogen show flat zoning profiles, which suggest homogenization by diffusion at high temperatures. Some other garnets are different with MgO decreasing and MnO increasing from core to rim suggesting late-stage retrograde Fe-Mg-Mn exchange (Jung and Mezger 2003). All garnets show no zoning with respect to the grossular component. Garnet from the meta-igneous migmatite sample 89.80 has a flat zoning profile. In contrast to the garnet from the metasedimentary migmatites, the garnet from the meta-igneous migmatite has low concentrations of MgO and MnO (Jung et al. 1999, 2000a). Garnet extracted from the granites of the Khan area shows similarities to garnet from the migmatites with either flat element distribution patterns (sample 98.297) or decreasing MgO and increasing MnO from core to rim (sample 98.298; Jung and Mezger 2003). Garnet from the late-tectonic granites from Oetmoed has distinctly higher MnO, but lower MgO concentrations relative to the migmatite garnets and is considered to be magmatic. There is a pronounced zonation with MnO increasing and MgO decreasing from core to rim (Jung et al. 1999, 2001). The garnets form the restite-bearing granite located at the road cut Omaruru-Kalkfeld differ from those at Oetmoed and the Khan river area. Generally, they have higher CaO and MgO, but lower MnO concentrations and have a core with a low grossular component and a broad rim enriched in grossular. Elemental profiles are generally flat, but there is a tendency for the pyrope component to decrease and the spessartine component to increase from core to rim (Jung et al. 2001).

Analytical techniques

The garnet was separated from a 40–80 mesh fraction. The sieved material was further processed with a magnetic separator and heavy liquids (methylen iodide). The final high-purity separates were produced by handpicking under a binocular microscope. Approximately 100–150 mg of garnet were washed in warm deionized water to remove surface contamination and then spiked with a mixed $^{205}Pb/^{235}U$ tracer before digestion in a mixture of concentrated HF and 7 N HNO_3 in 3-ml screw-top Teflon vials inside Krogh-style Teflon bombs at 200 °C for 5 days. After evaporation, the garnet was dissolved in 2.5 N HCl and loaded on Teflon columns filled with DOWEX AG 1X8 anion exchange resin (100–200 mesh) in chloride form (Mattinson 1986). Lead was separated using HCl-HBr chemistry, and U was separated using Eichrom resin and an improved 2 N HNO_3/0.02 N HNO_3 chemistry. Lead and U were loaded on Re single filaments following the H_3PO_4-silica gel method (Cameron et al. 1969). The procedural blank for the garnet analyses was between 22 and 56 pg and is considered to be negligible except for the analyses with low Pb concentrations. 30–50 mg of high-purity K-feldspar separates were washed with a mixture of 3:1 HCl/HNO_3 to remove surface contamination and then subsequently rinsed three times with ultrapure water. After this treatment the separates were leached three times in a mixture of concentrated HF/HNO_3 which resulted in a weight loss of ~70–80%. Subsequently, the feldspars were dissolved in concentrated HF and after evaporation redissolved in 2.5 N HCl and 0.6 N HBr and loaded on Teflon columns filled with DOWEX AG 1X8 anion exchange resin (100–200 mesh) in chloride form. The Pb was extracted using conventional HBr/HCl techniques and was loaded on Re single filaments following the H_3PO_4-silica gel method. The raw isotope ratios were corrected for mass fractionation with a factor of 0.12% per amu based on repeat analyses of the standard NBS SRM 982. The reproducibility of the standard NBS SRM 982 was 0.048, 0.029 and 0.077% for the $^{206}Pb/^{204}Pb$, $^{207}Pb/^{204}Pb$ and $^{208}Pb/^{204}Pb$ ratio, respectively. The total procedure blank < 100 pg Pb is negligible. Total blanks for U were < 30 pg and the U analyses were corrected for 0.04% per amu based on repeat analyses of the NBS U 500 standard. Uncertainties for the U/Pb and Pb/Pb ratios, ages and corresponding uncertainties were calculated using the programs PBDAT and ISOPLOT (Ludwig 1991a, 1991b).

Results

U-Pb systematics of monazite

Most monazite analyses from the Damara orogen yield slightly discordant ages (−1 to −3% reversely discordant; Briqueu et al. 1980; Kukla et al. 1991; Jung et al. 2001, Jung and Mezger 2003; this study). It is very common for monazite to yield reversely discordant U-Pb ages and it is widely accepted that this reverse discordance is the result of excess ^{206}Pb from the decay of initial ^{230}Th, a short-lived intermediate daughter isotope in the ^{238}U-^{206}Pb decay scheme (Schärer 1984). The $^{207}Pb/^{235}U$ age is not affected by this problem, and consequently can be regarded as the best estimate for the

Table 1 New Sm-Nd garnet-whole rock data from migmatized granites (Oetmoed; central Damara orogen, Namibia)

Sample	Locality	Rock type	Garnet type	$^{143}Nd/^{144}Nd$	$^{147}Sm/^{144}Nd$	Sm (ppm)	Nd (ppm)	Sm-Nd age
89.80 grt	Oetmoed	Granite	Migmatitic	515592 ± 28	1.176	0.418	0.215	487 ± 8
89.80 wr	Oetmoed	Granite		512286 ± 12	0.140	5.820	20.12	
89.19 grt	Oetmoed	Granite	Migmatitic	518610 ± 29	2.104	0.194	0.056	487 ± 4
89.19 wr	Oetmoed	Granite		512890 ± 12	0.312	1.690	3.280	

age of the monazites. The $^{207}Pb/^{235}U$ monazite ages from the metasedimentary migmatites from the Khan area range from 519 ± 1 to 530 ± 1 Ma (Jung and Mezger 2003). The granite sample 98.297 from the Khan area yielded a $^{207}Pb/^{235}U$ monazite age of 530 ± 1 Ma (Jung and Mezger 2003). The $^{207}Pb/^{235}U$ monazite ages from sample 89.80, the meta-igneous migmatite from the Oetmoed Migmatite Granite complex, average 528 ± 2 Ma, which is in agreement with the ages (526 ± 2–516 ± 2 Ma) obtained from unmigmatized samples from the same suite of granites (Jung et al. 2000a). The $^{207}Pb/^{235}U$ monazite ages from the restite-bearing granite from road cut Omaruru-Kalkfeld indicate growth of monazite between 511 ± 2 Ma and 518 ± 2 Ma (Jung et al. 2001).

Sm-Nd isotope systematics of garnet

Samarium-Nd garnet-whole rock ages for the meta-igneous and metapelitic migmatites from the Oetmoed Granite Migmatite Complex are identical for both samples (89.80:487 ± 8 Ma; 89.19:487 ± 4 Ma, Table 1), but substantially younger than the U-Pb monazite ages from sample 89.80 that range from 527 ± 2 to 529 ± 2 Ma (Table 2). Samarium-Nd ages calculated for garnet-whole rock pairs for the migmatites and the metasedimentary rock from the Khan area range from 523 ± 4 Ma to 512 ± 3 Ma and in most cases agree with the U-Pb monazite ages (530 ± 1–519 ± 1 Ma; Jung and Mezger 2003). For the granite sample 98.297 from the Khan area, the Sm-Nd age is 530 ± 3 Ma, which is identical to the U-Pb monazite age from this sample (Jung and Mezger 2003). Samarium-Nd garnet-whole rock pairs were also analysed on inferred magmatic garnets from the granites from the Oetmoed Granite Migmatite Complex (samples 89.52, 89.53, 12.2, 26.5). The resulting ages range from 484 ± 13 Ma to 492 ± 5 Ma (Jung et al. 2001). For these samples no monazite ages are available. For the samples from road cut Omaruru-Kalkfeld, Sm-Nd garnet-whole rock analyses yield indistinguishable ages between 488 ± 7 and 493 ± 6 Ma, again substantially younger than the Pb-Pb monazite ages (514 ± 1–516 ± 1 Ma; Jung et al. 2001).

U-Pb systematics of garnet

Uranium-Pb analyses were obtained following the method presented in the appendix. The U-Pb garnet data are presented in Table 2 and Fig. 2. Lead concentrations vary from 0.02 to 1.50 ppm, similar to Pb concentration in garnet reported previously (Mezger et al. 1989; Burton and O'Nions 1991; Vance and O'Nions 1990; Lanzirotti and Hanson 1995) but are mostly higher than the values reported by Vance et al. (1998) that range from 0.04–0.23 ppm. Uranium concentrations range from 0.25 to 2.55 ppm similar to values from other studies. Lead isotope compositions are highly variable with $^{206}Pb/^{204}Pb$ ratios mostly between 22 and 69. Only the garnets from the metapelitic migmatite sample 89.19 have significantly higher $^{206}Pb/^{204}Pb$ ratios between 205 and 613. $^{208}Pb/^{204}Pb$ ratios are also variable and range from ca. 38 for garnets from the late-tectonic granites from Oetmoed to 43–56 for garnets from the metasedimentary and meta-igneous migmatites. Garnet from the late-tectonic restite-bearing granite from road cut Omaruru-Kalkfeld has higher $^{208}Pb/^{204}Pb$ ratios up to 87. For garnets with very low $^{206}Pb/^{204}Pb$ ratios, an inappropriate estimation of the common Pb isotope composition at the time of garnet growth can significantly influence the degree of discordance and ultimately the ages, but cannot account for the magnitude of discordance observed here. However, in all cases the common Pb isotope composition of coexisting K-feldspar was used. K-feldspar has low U/Pb ratios and leaching K-feldspar with HF has been shown to remove preferentially the radiogenic component (Ludwig and Silver 1977; Housh and Bowring 1991). It is therefore suggested that the Pb isotope composition of leached K-feldspar reflects the isotope composition of the whole rock during the last thermal event. In Fig. 3, Pb-Pb garnet data are plotted together with the cogenetic K-feldspar from the same rock. It can be seen that the Pb isotope composition of the feldspar plots close to or on the regression line through the garnet data points. This feature indicates that garnet and K-feldspar are cogenetic with respect to the Pb isotope composition and have undergone their U-Pb fractionation at the same time. However, diffusivities for Pb in K-feldspar and garnet are different and therefore, the measured Pb isotope composition of K-feldspar may slightly differ from those at the time of garnet growth. The most notable exception in Fig. 3 are the garnet data from the Khan area. Here, the plotted garnet fractions represent single analyses of bulk garnet from different rocks and the resulting scatter is probably the result of the different episodes of garnet growth in the host rocks. The general agreement of the garnet-K-feldspar ages and the Sm-Nd garnet ages despite the relatively large range in

Table 2 U-Pb monazite and garnet data from migmatites and granites (central Damara orogen, Namibia)

Sample	89.80	89.80	89.80	12.2.2	26.5.2	89.52.2	89.52.3	89.52.4	89.53.1	89.53.2	89.53.3	89.80.1	89.80.2	89.80.3
Mineral	Mnz	Mnz	Mnz	Grt	Grt	Grt	Grt	Grt	Grt	Grt	Grt	Grt	Grt	Grt
Locality	Oetmoed	Oetmoed	Oetmoed	Oetmoed	Oetmoed	Oetmoed	Oetmoed	Oetmoed	Oetmoed	Oetmoed	Oetmoed	Oetmoed	Oetmoed	Oetmoed
Host rock	Granite	Granite	Granite	Granite	Granite	Granite	Granite	Granite	Granite	Granite	Granite	Granite	Granite	Granite
Garnet type				Igneous	Igneous	Igneous	Igneous	Igneous	Igneous	Igneous	Igneous	Migmatitic	Migmatitic	Migmatitic
U (ppm)	5080	4144	5220	1.316	0.434	0.580	1.772	0.936	2.427	2.296	1.475	2.201	1.945	2.487
Pb (ppm)	937	761	962	0.307	0.711	0.350	0.642	0.576	0.613	0.791	0.610	1.123	1.093	1.316
Th/U	4.6	4.6	4.6	0.6	1.8	1.5	0.7	0.9	0.7	0.5	0.8	1.1	1.1	1.4
U/Pb	5.4	5.4	5.4	4.3	0.6	1.7	2.8	1.6	4.0	2.9	2.4	2.0	1.8	1.9
$^{208}Pb/^{204}Pb$	12118	12620	12692	37.84	0.4518	0.7126	0.3941	0.2878	0.0683	0.2475	0.4272	15.09	14.07	24.02
$^{206}Pb/^{204}Pb$	8552	8905	8954	53.70	24.40	27.55	47.80	39.05	48.62	62.13	45.19	67.21	65.08	69.45
$^{208}Pb/^{206}Pb$	1.4170	1.4171	1.4174	0.00382	0.01851	0.02587	0.00824	0.00737	0.00140	0.00398	0.00945	0.22449	0.21617	0.34590
$^{207}Pb/^{206}Pb$	0.05765	0.05769	0.05771	0.05726	0.05670	0.05689	0.05667	0.05656	0.05670	0.05645	0.05674	0.05677	0.05701	0.05697
Error	0.00003	0.00003	0.00003	0.00102	0.00362	0.00235	0.00079	0.00112	0.00105	0.00050	0.00081	0.00048	0.00048	0.00044
$^{207}Pb/^{235}U$	0.68323	0.68097	0.68338	0.68326	1.15564	0.61669	0.93364	1.22436	0.66453	1.14549	0.99694	1.65603	1.79157	1.68912
Error	0.00155	0.00128	0.00163	0.0133	0.07754	0.02682	0.01412	0.02583	0.01410	0.01104	0.01512	0.01552	0.01765	0.01550
$^{206}Pb/^{238}U$	0.08595	0.08561	0.08588	0.08655	0.14781	0.07861	0.11950	0.15700	0.08500	0.14716	0.12744	0.21156	0.22790	0.21505
Error	0.00032	0.00030	0.00033	0.00042	0.00087	0.00042	0.00060	0.00080	0.00075	0.00060	0.00052	0.00086	0.00122	0.00115
Ages (Ma)														
$^{206}Pb/^{238}U$	532	530	531	535	889	488	728	940	526	885	773	1237	1324	1256
$^{207}Pb/^{235}U$	529	527	529	529	780	488	670	812	517	775	702	992	1042	1004
$^{207}Pb/^{206}Pb$	517	518	519	501	480	487	479	474	480	470	481	483	492	490
Feldspar														
$^{206}Pb/^{204}Pb$				18.439	18.244	18.212			18.232			18.792		
$^{207}Pb/^{204}Pb$				15.626	15.618	15.615			15.627			15.712		
$^{208}Pb/^{204}Pb$				37.854	37.775	37.740			37.839			37.983		

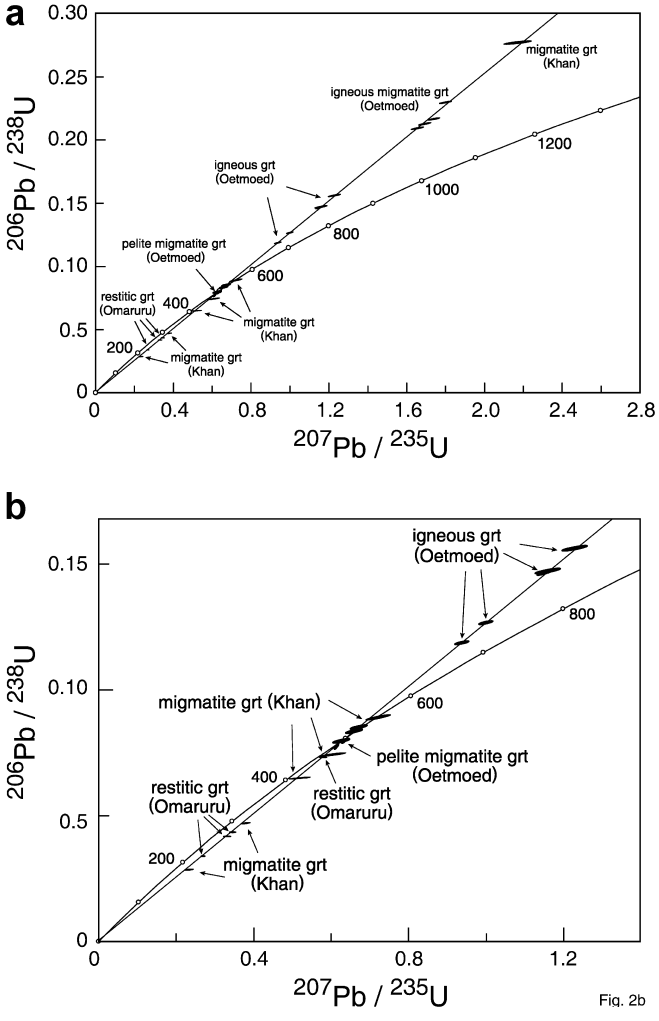

$^{206}Pb/^{204}Pb$ ratios indicates that the common Pb correction applied to the garnet is broadly correct. One notable feature of the garnet U-Pb analyses is their strong negative or positive discordance in a concordia diagram (Fig. 2). Igneous garnet from the late-tectonic granites at Oetmoed is either nearly concordant or strongly reverse discordant whereas the meta-igneous migmatites at Oetmoed are strongly reverse discordant. Similarly, the migmatite samples from the Khan area are either concordant or strongly reverse discordant (Fig. 2). Reverse discordance may arise from loss of U or excess ^{206}Pb from the decay of excess initial ^{230}Th (Schärer 1984). Uranium is located in the crystal structure of garnet (see discussion in Mezger et al. 1989) and loss of U is therefore considered to be unlikely. The magnitude of reverse discordance is too large to be related to ^{230}Th-related excess. On the other hand, samples from the late-tectonic restite-bearing granite from roadcut Omaruru-Kalkfeld are either nearly concordant or strongly normal discordant (0.8 to 11% discordant). Discordance may result from U gain or Pb loss during volume diffusion, however, there is no clear relationship between U/Pb ratio, Pb concentration and discordance. It is noteworthy that the U/Pb ratios of the nearly concordant samples cover the full range of U/Pb ratios observed in the discordant samples. Most analyses were duplicated, and in some cases the duplicate represents

◄

Fig. 2 **a** U-Pb concordia plot for the different garnets. Note the general agreement of the Pb-Pb ages despite the strong discordance of many samples probably due to a recent laboratory-induced fractionation of U from Pb. **b** Enlargement of **a** to show the location of the concordant and discordant samples in more detail

89.80.4 Grt Oetmoed Granite Migmatitic	89.19.1 Grt Oetmoed Granite Migmatitic	89.19.2 Grt Oetmoed Granite Migmatitic	89.19.3 Grt Oetmoed Granite Migmatitic	89.19.4 Grt Oetmoed Granite Migmatitic	K 4.1 Grt Khan Migmatitic Migmatitic	K 4.2 Grt Khan Migmatitic Migmatitic	K 4.5 Grt Khan Metased. Migmatitic	K 4.7 Grt Khan Migmatitic Migmatitic	94.297 Grt Khan Granite Migmatitic	94.298 Grt Khan Granite Migmatitic	S 84.1 Grt Omaruru Granite Restitic	S 84.2 Grt Omaruru Granite Restitic	S 85.1 Grt Omaruru Granite Restitic	S 85.2 Grt Omaruru Granite Restitic
2.441	0.346	0.737	0.253	0.284	0.684	2.550	0.506	0.959	0.998	0.317	1.505	1.093	2.220	2.043
1.372	0.035	0.059	0.025	0.026	1.331	1.501	0.127	1.400	0.241	0.458	0.288	0.360	0.306	0.337
1.5	0.2	0.1	0.2	0.2	3.62	4.04	2.83	3.01	1.85	1.32	2.45	2.36	3.96	3.89
1.8	10.0	12.4	10.3	11.0	0.51	1.70	3.99	0.69	4.15	0.69	5.22	3.04	7.26	6.07
25.35	6.118	14.04	6.632	10.91	35.36	43.68	30.51	21.21	6.419	2.513	28.40	27.11	70.01	73.35
67.56	205.36	613.23	253.82	375.50	21.52	28.37	36.22	22.42	27.32	32.71	40.15	40.51	52.45	56.59
0.37524	0.02979	0.02289	0.02613	0.02906	1.643144	1.539295	0.842305	0.946066	0.234958	0.076824	0.70735	0.66914	1.33476	1.29625
0.05692	0.05703	0.05702	0.05720	0.05739	0.05862	0.05734	0.05811	0.05877	0.05795	0.05691	0.05704	0.05727	0.05738	0.05721
0.00046	0.00014	0.00006	0.00016	0.00008	0.00663	0.00225	0.00124	0.00591	0.00240	0.00147	0.00102	0.00106	0.00066	0.00079
1.74102	0.61510	0.61208	0.63149	0.64103	0.72431	0.52212	0.38305	0.60795	0.23815	2.17144	0.33561	0.58862	0.27520	0.34984
0.01652	0.00217	0.00164	0.00242	0.00183	0.08628	0.02157	0.00863	0.06438	0.01040	0.05896	0.00638	0.01161	0.00341	0.00507
0.22183	0.07822	0.07785	0.08007	0.08101	0.08961	0.06604	0.04781	0.07502	0.02981	0.27675	0.04268	0.07455	0.03479	0.04435
0.00118	0.00031	0.00030	0.00031	0.00032	0.00075	0.00031	0.00020	0.00058	0.00014	0.00117	0.00017	0.00031	0.00014	0.00018
1292	485	483	497	502	553	412	301	466	189	1575	269	464	220	280
1024	487	485	497	503	553	427	329	482	217	1172	294	470	247	305
489	493	492	499	506	553	505	534	559	528	488	493	502	506	500
	18.400				18.284	18.788	18.400	18.840	18.253	17.900	18.705		18.785	
	15.640				15.655	15.676	15.640	15.669	15.654	15.704	15.645		15.636	
	37.800				38.060	38.750	38.440	38.490	37.880	38.240	38.025		38.062	

another batch of the same mineral separate (samples 89.80, 89.19, S 82, S 84). For these samples, the $^{207}Pb/^{206}Pb$ ages agree within analytical uncertainty. For samples where a different mineral separate was used, the ages usually do not agree within analytical uncertainty, but are similar within 10%. All replicate analyses indicate that the discordance is variable although there is general agreement in the $^{207}Pb/^{206}Pb$ ages suggesting that the discordance is recent. We prefer the explanation given by Mezger et al. (1989) that during analyses significant changes of the U/Pb ratios took place, most probably due to the high viscosity of the solution, which makes homogenization between spike and sample difficult. Therefore, the Pb and U concentration of the discordant samples are only approximate values.

Discussion

Comparison of Sm-Nd and U-Pb garnet ages: the influence of inclusions

Small inclusions of REE- and U-rich minerals (allanite, monazite, zircon) may influence U-Pb and Sm-Nd garnet ages, however, the critical constraint is that duplicate analyses of the same garnet yield reproducible ages although these garnet fractions show a considerable spread in U/Pb ratios (Fig. 4). This feature indicates that the garnet and the inclusions were separated from the matrix at the same time and that this time is most likely the time of garnet growth. Alternatively, it is probable that the Sm-Nd isotope system of the inclusions has been reset and equilibrated during garnet growth. The most notable feature of the Sm-Nd garnet analyses is the observation that the leached garnets have significantly less Sm and Nd but higher Sm/Nd than the unleached garnets. Some of the higher values approach the Sm and Nd concentrations in garnet reported in the literature (Henson and Zhou 1995; Maboko and Nakamura 1995; Moyes and Groenewald 1996; Stowell and Goldberg 1997), although there are also numerous examples of even higher Sm and Nd concentrations (Zhou and Henson 1995; DeWolf et al. 1996; Moyes and Groenewald 1996). The low concentrations from the strongly leached samples are similar to the values obtained by ion microprobe studies (Hickmott et al. 1987; Harris et al. 1992; Sevigny 1993) and laser-ablation ICP-MS studies (Prince et al. 2000). It is suggested that analyses with high Nd concentrations, low $^{147}Sm/^{144}Nd$ ratios and hence unradiogenic $^{143}Nd/^{144}Nd$ ratios indicate contamination with minute LREE-rich inclusions (Jung and Mezger 2001, 2003; Jung et al. 2001). It has been previously shown that chemical leaching induces no apparent artefact on Sm-Nd garnet ages (Henson and Zhou 1995; DeWolf et al. 1996; Jung et al. 2000a, Jung and Mezger 2001). The chemical leaching method effectively removes most of the monazite and apatite inclusions, but fails to eliminate zircon from the garnet sample. The presence of inherited Sm-Nd isotope systematics in zircon (e.g., Paterson et al. 1992) has probably no significant effect for Sm-Nd garnet geochronology, as long as the included zircon is not too old, because zircon also has elevated Sm/Nd ratios but low Nd concentrations.

Figure 5a shows $^{208}Pb/^{204}Pb$ vs. $^{206}Pb/^{204}Pb$ isotope ratios of the analyzed garnet fractions. Garnet from the pelitic migmatite sample 89.19 and the late tectonic granites at Oetmoed have a large range in $^{206}Pb/^{204}Pb$

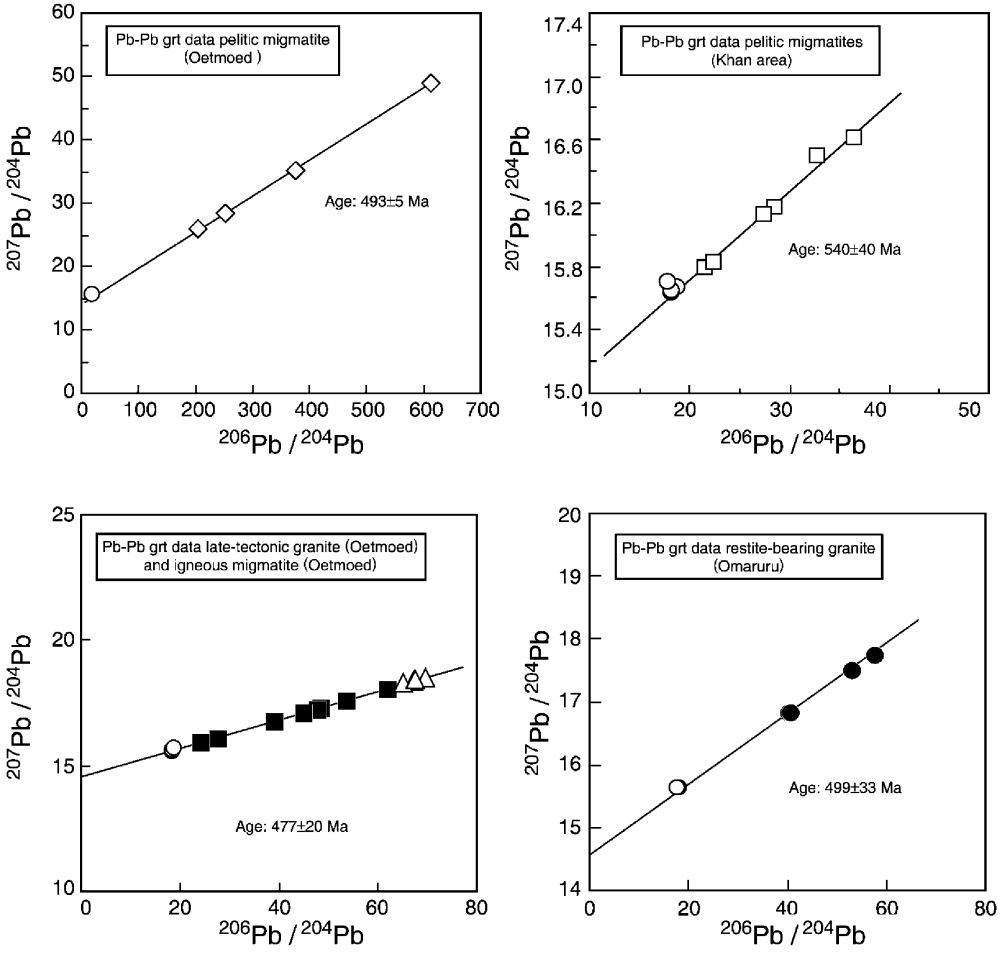

Fig. 3 Plot of $^{207}Pb/^{204}Pb$ vs. $^{206}Pb/^{204}Pb$ for the different garnets

ratios (and corresponding high U/Pb ratios) and only moderate high $^{208}Pb/^{204}Pb$ ratios. The high $^{206}Pb/^{204}Pb$ ratios of garnet from sample 89.19 indicate that the Pb isotope composition of this garnet is dominated by zircon inclusions and the slightly elevated $^{208}Pb/^{204}Pb$ ratios can be explained by some additional influence of monazite inclusions. Garnet from the late tectonic granites at Oetmoed is less affected by zircon and monazite inclusions. The other garnet fractions show are larger variation in $^{208}Pb/^{204}Pb$ at low $^{206}Pb/^{204}Pb$ ratios suggesting that in this case monazite may have controlled the Pb isotope composition. A similar conclusion can be drawn from Fig. 5b in which these garnet fractions show high Th/U ratios (calculated from Pb isotope composition) and high $^{208}Pb/^{204}Pb$ ratios. The suggestion that different $^{208}Pb/^{204}Pb$, $^{206}Pb/^{204}Pb$ and corresponding Th/U ratios are caused by different amounts of zircon and monazite is corroborated by BSE images of the different garnet species (Fig. 6). It is evident that sample 89.19 (pelitic migmatite garnet, Oetmoed) which has high $^{206}Pb/^{204}Pb$ ratios and low Th/U ratios is dominated by inclusions of zircon whereas sample S 85 (restitic garnet, Omaruru) and sample 89.80 (igneous migmatite, Oetmoed) which have high $^{208}Pb/^{204}Pb$ and high Th/U ratios are contaminated by monazite. Sample 89.80 (igneous migmatite garnet, Oetmoed) and the samples from the Khan area show the influence of both accessory minerals, zircon and monazite.

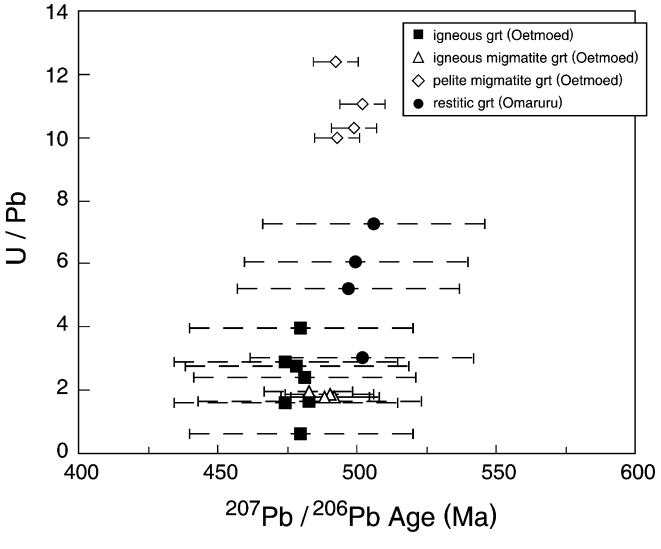

Fig. 4 Plot of U/Pb ratio vs. $^{207}Pb/^{206}Pb$ age of the different garnet fractions. Note the general similarity of the $^{207}Pb/^{206}Pb$ ages for each group despite the range in U/Pb ratios

Trace element ratios (e.g., Th/U, Nd/U, Sm/Nd; DeWolf et al. 1996) have been used to show whether the

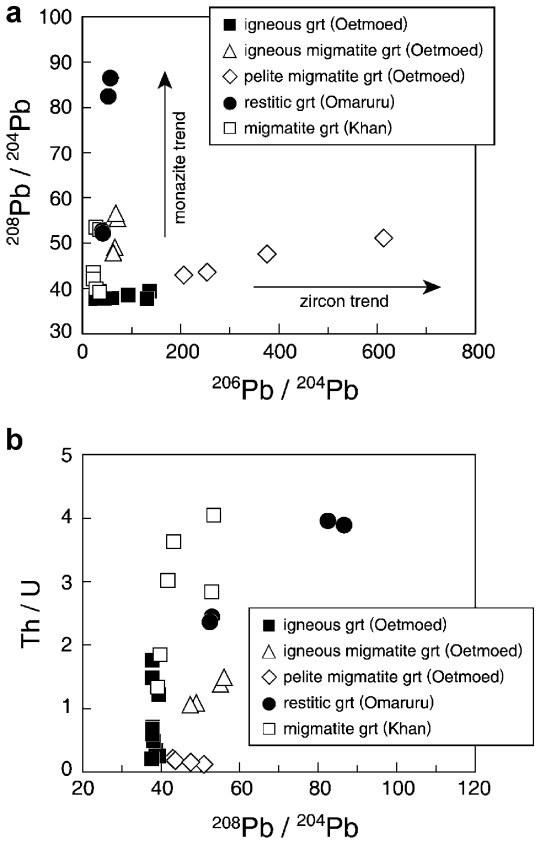

Fig. 5 Plot of **a** $^{208}Pb/^{204}Pb$ vs. $^{206}Pb/^{204}Pb$ and **b** Th/U vs. $^{208}Pb/^{204}Pb$ for the different garnets

trace elements Sm, Nd, U and Th are hosted in the garnet structure itself or in inclusions of zircon, monazite or allanite. Such an evaluation is important, because zircon and monazite can survive previous episodes of high-grade metamorphism and may therefore record a premetamorphic Pb signature. Figure. 7a, b show diagrams of Nd/U vs. Th/U and U/Nd vs. Sm/Nd for the different garnet fractions. Monazite and allanite have typically Th/U $\gg 3$ while zircon has Th/U $\ll 1$ (DeWolf et al. 1996). Uranium/Nd and Sm/Nd ratios for zircon may vary widely, however, the majority of data indicate U/Nd ratios ranging from ca. 10 to 1,000 and corresponding Sm/Nd ratios between 0.5 and 3 (DeWolf et al. 1996). Ionprobe and geochronological studies obtained on zircon indicate U/Nd ratios between ca. 300 and 3,000 with corresponding Sm/Nd ratios of ca. 2 for this mineral (Poller et al. 2001). Th/U ratios are low in garnet ($\ll 1$; DeWolf et al. 1996). Additionally, garnet bulk composition can have a considerable control over trace element abundances and ratios. DeWolf et al. (1996) have shown that andradite-rich garnets may have higher concentrations of REE, Th and U than almandine-pyrope rich garnets due to the substitution of Fe^{3+} for Al^{3+} which permits increased substitution of the large cations Sm, Nd, Th and U. Therefore, an evaluation of Th/U and Sm/Nd ratios alone may not be useful to detect the presence of inclusions. In the present study only almandine-rich garnets have been investigated and the effect of garnet bulk composition in controlling Sm, Nd, Th and U abundances is likely similar for all samples. Variation in Th/U, Nd/U and Sm/Nd ratios between the different garnet species may therefore be interpreted as the result of two- or three-component mixture between garnet and monazite/allanite and zircon.

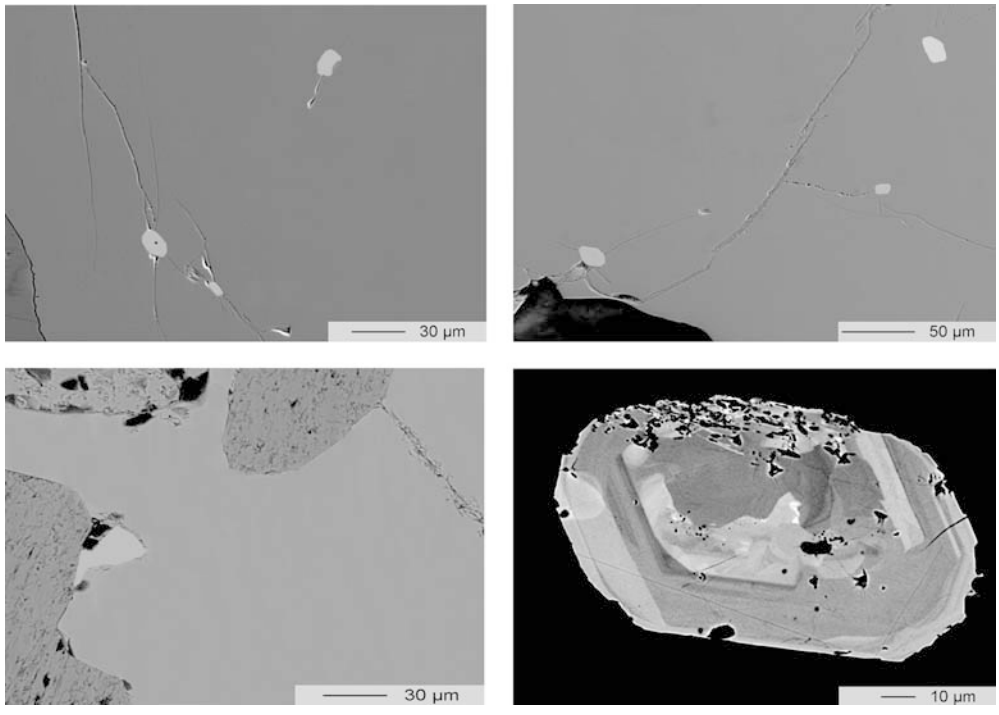

Fig. 6 Back-scattered electron imaging of garnet (*dark grey*) showing tiny inclusions of monazite (*brighter grains*) and zircon (*less brighter grains*). Garnet (*upper left*) from pelitic migmatite (Oetmoed) with inclusions of zircon only, restitic garnet (*lower left*) from Omaruru with inclusion of monazite only. *Large inclusions with rough surfaces* are biotite, garnet (*upper right*) from igneous migmatite (Oetmoed) with inclusions of monazite and zircon, BSE image of matrix monazite (*lower right*) from igneous migmatite (Oetmoed) with simple concentric growth zonation implying a magmatic origin for these monazites

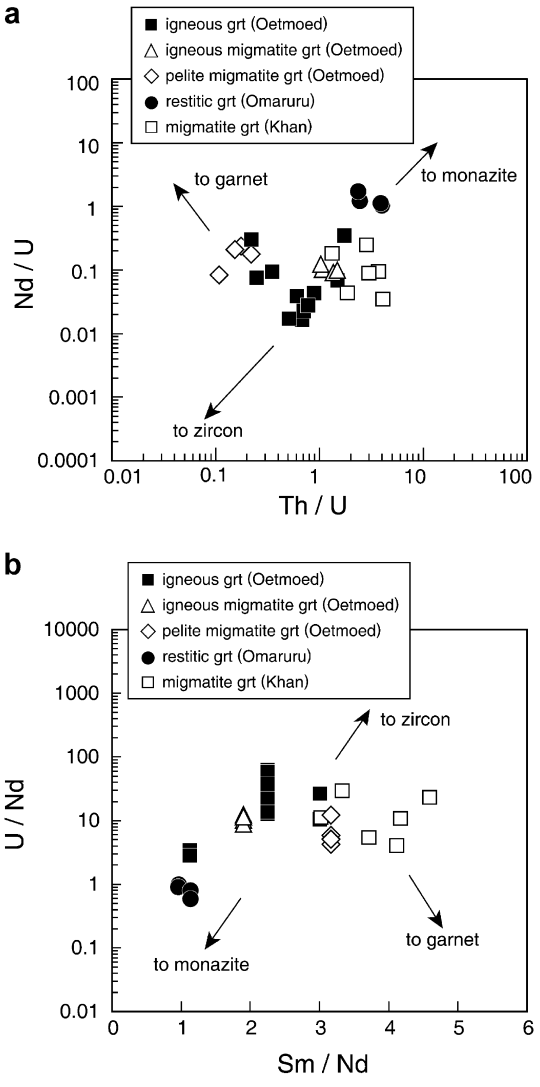

Fig. 7 Plot of **a** Nd/U vs. Th/U and **b** U/Nd vs. Sm/Nd for the different garnets

Consistency of U-Pb garnet and monazite and Sm-Nd garnet ages

The Sm-Nd whole rock-garnet and U-Pb monazite ages obtained from the metasedimentary migmatites and some syntectonic granites range from ca. 530 to 510 Ma. This feature suggests a prolonged growth history in which the different garnet ages are interpreted to reflect distinct stages of garnet growth during high-grade metamorphism. The ages for the growth of monazite within the Pan-African Damara orogen apparently record three distinct episodes at ca. 540–530 Ma, 520–500 Ma and 480–470 Ma without resetting of the older ages (Briqueu et al. 1980; Kukla et al. 1991; Jung et al. 2000a, 2001; Jung and Mezger 2001). Similarly, Sm-Nd whole rock garnet ages record these events without any sign of resetting of the older ages (Jung et al. 2000b; Jung and Mezger 2001, 2003). Previous studies have shown that replicate analyses of monazite from the same sample (e.g., Jung and Mezger 2001) gave identical ages, suggesting that resetting of the monazite late in the metamorphic history is unlikely, since it is unlikely that all grains in a sample are reset to the same amount. It is also unlikely because for these analyses 2–4 grains or even one large grain were used. In the metasedimentary migmatites from the Khan area, Sm-Nd garnet ages appear to be slightly younger than U-Pb monazite ages from the same rock. Peak metamorphic temperatures reached ca. 750 °C in this area (Jung and Mezger 2003) and therefore, the younger Sm-Nd garnet ages may simply reflect the lower closure temperature for Sm-Nd in garnet than for U-Pb in monazite. However, the difference is typically less than 10 Ma (Jung and Mezger 2003). Alternatively, monazite and garnet were produced at different times. The generation of the migmatites in the Khan area is related to intrusion of granitic melts, therefore, the younger Sm-Nd ages most likely reflect the ages of garnet growth coeval with intrusion of melts shortly after the peak of regional metamorphism. In contrast to the more classical approach to blocking temperatures which involves an assessment of the diffusion rate, grain size and the crystal geometry and composition, there is growing evidence that the presence or absence of a fluid phase during metamorphism and melting, accompanied by penetrative deformation, can significantly alter the diffusion rates at constant temperature, thus affecting the blocking temperature and ultimately the ages (Mork and Means 1986; Erambert and Austrheim 1993). A closure temperature of >800 °C has been proposed for the U-Pb system in garnet (Mezger et al. 1989) and consequently, utilizing the U-Pb system in garnet may be the most successful way to determine mineral growth ages from high grade terranes. For the migmatite garnets from the Khan area $^{207}Pb/^{206}Pb$ garnet ages have large errors due to their low $^{206}Pb/^{204}Pb$ ratios but they appear to be older or similar to the $^{207}Pb/^{235}U$ monazite ages. They appear mostly also older than the Sm-Nd whole rock garnet ages from the same sample. These features suggest that the closure temperature of U-Pb in garnet is similar or slightly higher than for monazite, but is higher than for Sm-Nd. In the meta-igneous and metapelitic migmatite from Oetmoed with estimated peak temperatures of ca. 730 °C (Table 3), both the Sm-Nd and U-Pb garnet ages are similar and younger than the U-Pb monazite ages, which seems surprising given the empirical observation that the closure temperature for U-Pb in garnet and monazite are probably similar and higher than 800 °C (Mezger et al. 1989; Parrish 1990) whereas the closure temperature for Sm-Nd in garnet is lower, probably around 650 °C (Mezger et al. 1992). Unmigmatized granite samples lacking garnet from the same outcrop yielded $^{207}Pb/^{235}U$ monazite ages between 516 ± 1 and 526 ± 1 Ma (Jung et al. 2000a) similar to the monazite age from the meta-igneous migmatite sample 89.80 (527–529 ± 2 Ma, this study). It is therefore proposed that the U-Pb monazite ages date the intrusion of the granite. Fig. 6 shows a BSE image of matrix monazite from this sample with a simple concentric zoning pattern suggesting magmatic growth for this type of monazite. Later in the metamorphic

Table 3 Overview of thermobarometric and geochronological data from migmatites and granites (central Damara orogen, Namibia). *n.a.* Not available

Sample	Locality	Rock type	Garnet type	P/T	Sm-Nd grt age	Pb-Pb grt age	U-Pb mnz age	Ref.
K 4.1	Khan	Migmatite	Migmatitic	710 °C/5.0	512 ± 3	553 ± 61	519 ± 1	Jung and Mezger (2003), this study
K 4.2	Khan	Migmatite	Migmatitic	700 °C/5.0	518 ± 3	505 ± 20	517 ± 1	Jung and Mezger (2003), this study
K 4.7	Khan	Migmatite	Migmatitic	700 °C/5.4	523 ± 4	534 ± 11	530 ± 1	Jung and Mezger (2003), this study
K 4.5	Khan	Metapelite	Metamorphic	590 °C/7.0	509 ± 4	559 ± 60	523 ± 1	Jung and Mezger (2003), this study
94.297	Khan	Granite	Migmatitic	670 °C/5.7	530 ± 3	528 ± 28	530 ± 1	Jung and Mezger (2003), this study
94.298	Khan	Granite	Migmatitic	690 °C/4.7	469 ± 3	488 ± 13	n.a.	Jung and Mezger (2003), this study
S 84.1	Omaruru	Granite	Restitic	800 °C/10	493 ± 6	493 ± 9	514 ± 1	Jung et al. (2001), this study
S 84.2	Omaruru	Granite	Restitic	800 °C/10	493 ± 6	502 ± 9	514 ± 1	Jung et al. (2001), this study
S 85.1	Omaruru	Granite	Restitic	820 °C/11	488 ± 7	506 ± 6	516 ± 1	Jung et al. (2001), this study
S 85.2	Omaruru	Granite	Restitic	820 °C/11	488 ± 7	500 ± 7	516 ± 1	Jung et al. (2001), this study
12.2.1	Oetmoed	Granite	Igneous	720 °C/6.0	486 ± 4	476 ± 13	n.a.	Jung et al. (2001), this study
12.2.2	Oetmoed	Granite	Igneous	720 °C/6.0	486 ± 4	501 ± 9	n.a.	Jung et al. (2001), this study
26.5.1	Oetmoed	Granite	Igneous	740 °C/6.0	484 ± 13	499 ± 2	n.a.	Jung et al. (2001), this study
26.5.2	Oetmoed	Granite	Igneous	740 °C/6.0	484 ± 13	480 ± 30	n.a.	Jung et al. (2001), this study
89.52.1	Oetmoed	Granite	Igneous	815 °C/6.5	492 ± 5	473 ± 6	n.a.	Jung et al. (2001), this study
89.52.2	Oetmoed	Granite	Igneous	815 °C/6.5	492 ± 5	487 ± 20	n.a.	Jung et al. (2001), this study
89.52.3	Oetmoed	Granite	Igneous	815 °C/6.5	492 ± 5	479 ± 7	n.a.	Jung et al. (2001), this study
89.52.4	Oetmoed	Granite	Igneous	815 °C/6.5	492 ± 5	474 ± 9	n.a.	Jung et al. (2001), this study
89.53.1	Oetmoed	Granite	Igneous	760 °C/6.0	489 ± 7	480 ± 9	n.a.	Jung et al. (2001), this study
89.53.2	Oetmoed	Granite	Igneous	760 °C/6.0	489 ± 7	470 ± 4	n.a.	Jung et al. (2001), this study
89.53.3	Oetmoed	Granite	Igneous	760 °C/6.0	489 ± 7	481 ± 7	n.a.	Jung et al. (2001), this study
89.80.1	Oetmoed	Granite	Migmatitic	730 °C/6.3	487 ± 8	483 ± 4	528 ± 1	Jung and Mezger (this study)
89.80.2	Oetmoed	Granite	Migmatitic	730 °C/6.3	487 ± 8	492 ± 4	528 ± 1	Jung and Mezger (this study)
89.80.3	Oetmoed	Granite	Migmatitic	730 °C/6.3	487 ± 8	490 ± 4	528 ± 1	Jung and Mezger (this study)
89.80.4	Oetmoed	Granite	Migmatitic	730 °C/6.3	487 ± 8	489 ± 4	528 ± 1	Jung and Mezger (this study)
89.19.1	Oetmoed	Granite	Migmatitic	720 °C/9.0	487 ± 4	493 ± 1	n.a.	Jung and Mezger (this study)
89.19.2	Oetmoed	Granite	Migmatitic	720 °C/9.0	487 ± 4	492 ± 1	n.a.	Jung and Mezger (this study)
89.19.3	Oetmoed	Granite	Migmatitic	720 °C/9.0	487 ± 4	499 ± 1	n.a.	Jung and Mezger (this study)
89.19.4	Oetmoed	Granite	Migmatitic	720 °C/9.0	487 ± 4	500 ± 1	n.a.	Jung and Mezger (this study)

history at ca. 490 Ma, migmatization during high-grade metamorphism produced the garnet at temperatures of ca. 730 °C (Jung et al. 2000a), a temperature too low to reset the monazite. In this case, the U-Pb and Sm-Nd garnet ages represent true growth ages. The similarity of the U-Pb and Sm-Nd garnet ages imply fast cooling at the end of the Pan-African orogeny in the central Damara orogen. The thermal circumstances that caused migmatization of metapelitic and meta-igneous rocks are probably related to the intrusion of hot, water-undersaturated melts into the terrane (Jung et al. 2000b). The Pb-Pb ages obtained on garnets from the late-tectonic granites at Oetmoed are similar to the Sm-Nd garnet-whole rock ages (Jung et al. 2001). These inferred magmatic garnets have euhedral shapes and pronounced major element zonations from core to rim. The preservation of magmatic garnets suggests that they crystallized at high temperatures (Jung et al. 2001) and low $a\ H_2O$ (Clemens and Wall 1988). The preservation of major element zonation and the similarity of U-Pb and Sm-Nd ages suggests that both ages represent also true growth ages, because no later recrystalisation and diffusion occurred after ca. 470 Ma (Jung 2001). Thus, the similarity of Pb-Pb and Sm-Nd garnet ages indicate fast cooling after intrusion of the melts. For the late tectonic granites from road cut Omaruru Kalkfeld, U-Pb monazite ages are older than the Sm-Nd and U-Pb garnet ages. This granite is undeformed and unmigmatized and intruded into a terrane with regional metamorphic temperatures not exceeding ca. 650°C. Garnet textures, CaO zonation and P-T estimates (9–10 kbar/800 °C; Jung et al. 2001) suggest that these garnets represent entrained material from the lower crustal source region. Whole rock analyses and the monazite and garnet data indicate an environment with a high Th/U ratio and it is suggested that the source region underwent U depletion due to granulite facies conditions during previous metamorphic episodes. The monazite ages between 520 and 510 Ma are interpreted as the peak of regional metamorphism (see also Jung 2001) of the deep crustal source and consequently the monazite is interpreted to represent entrained material from that source. The entrained garnet was also part of that source, but formed during a later stage of regional metamorphism and melting. The similarity between Sm-Nd and U-Pb ages indicates the time of rapid melt extraction and intrusion, 10–30 Ma after the peak of regional metamorphism.

Summary and conclusions

Implications for the interpretation of Sm-Nd garnet ages in high-grade terranes

Previous results from extensive leaching procedures (e.g. Jung and Mezger 2001, 2003) have shown that leaching

induces no apparent artefact on Sm-Nd systematics of garnet and can be used to test for monazite inclusions. Because all of the garnet fractions treated in this study show increasing Sm/Nd ratios with increasing leaching intensity (Jung et al. 2001; Jung and Mezger 2003) inclusions of monazite are apparently important. The presence of monazite inclusions in garnet has a marked influence on Sm and Nd concentrations and may result in initial isotopic disequilibrium, if the closure temperature for isotopic exchange of Nd is higher in monazite than in garnet. However, volume diffusion for Nd in monazite is expected to be very small and even if isotopic equilibrium is not achieved, this may have a negligible effect on garnet-whole rock systematics because the Sm/Nd fractionation between monazite and whole rock is expected to be very small. The presence of zircon inclusions may cause some deviation from a garnet-whole rock Sm-Nd isochron age due to the apparently common occurrence of inherited Nd isotope systematics in zircon (e.g. Paterson et al. 1992; von Quadt 1992; von Blanckenburg 1993) and the large fractionation in Sm/Nd relative to the whole rock. However, Nd concentrations in zircon are expected to be small and therefore, inclusions of zircon are expected to have little influence on garnet Sm-Nd isochrons. This study has demonstrated that in some garnets, U is hosted primarily in inclusions. Analysing different fractions of the same garnet population for Sm-Nd and U-Pb together with U-Pb analyses of monazite from the same rock, coupled with inspection of trace element ratios provides criteria for evaluating the role of inclusions in the U and radiogenic Pb budget of metamorphic garnets. If trace element ratio variation indicates the presence of inclusions, then the use of U-Pb garnet ages requires an understanding of the genetic relationships between the garnet and the inclusion phases.

Garnets from pelitic migmatites that have undergone medium pressure granulite facies metamorphism of ca. 750 °C/5–6 kbar (Khan area, Damara orogen, Namibia) record Pb-Pb ages between ca. 550 and 520 Ma that appear to be slightly older or similar to U-Pb monazite and Sm-Nd garnet whole rock ages. These garnets have very low $^{206}Pb/^{204}Pb$ ratios. Together with the uncertainty of the initial Pb isotope composition large errors are associated with these analyses. However, it is reasonable to assume that in this case the garnet ages define growth ages, probably related to the first peak of high-grade metamorphism in this part of the orogen.

For an igneous migmatite sample from Oetmoed, Pb-Pb garnet and Sm-Nd garnet whole rock ages are similar (ca. 490 Ma), whereas the matrix monazite from the same sample is ca. 40 Ma older than the garnet. The monazite ages are similar to monazite ages from unmigmatized granite samples and constrain precisely the intrusion of the precursor granite in this area. Although there is a notable difference in closure temperature for the U-Pb and Sm-Nd system in garnet, the similarity of both ages indicate that both garnet ages record garnet growth in a migmatitic environment.

Garnet fractions from a pelitic migmatite show high $^{206}Pb/^{204}Pb$ ratios indicating the presence of zircon inclusions. However, the Pb-Pb ages are also similar to or only slightly older than the Sm-Nd garnet-whole rock ages implying that in this case the zircon is also not very much older than the garnet. Despite the apparent difference in closure temperature for the U-Pb and Sm-Nd system in garnet, the similarity of both ages implies that after ca. 490 Ma no significant thermal overprint occurred in the Pan-African Damara orogen of Namibia. In both cases, the similarity between the Pb-Pb and Sm-Nd garnet ages implies that the included monazite and zircon do not induce a premetamorphic Pb signature upon the garnet.

For restitic garnets from an unmigmatized granite at Omaruru, Pb-Pb and Sm-Nd garnet ages are also similar, but 10–25 Ma younger than U-Pb monazite ages from the same sample. Whereas the monazite ages define probably the peak of regional metamorphism in the source of the granite (e.g. Jung 2001), the garnet ages likely indicate the time of melt extraction. Difference in Pb-Pb garnet and monazite ages can be explained by the fact that monazite is likely resistant to later thermal re-equilibration in the temperature range between 750 and 900 °C and is therefore capable of recording earlier intrusive or regional metamorphic events.

For magmatic garnets that record higher temperatures (Jung et al. 2001) than the metamorphic country rock in which they intruded, the similarity between Pb-Pb and Sm-Nd garnet ages is consistent with fast cooling rates of granitic dykes in the lower to middle crust. Overall, the Pb-Pb garnet ages usually agree with the Sm-Nd garnet-whole rock ages from the same sample.

Implications for the role of high U/Th inclusions

This study has shown that garnets from igneous and pelitic migmatites and granites have moderately high concentrations of Pb (0.02–1.50 ppm) and U (0.25–2.55 ppm). A recent laboratory-induced discordance is observed and a correction for U fractionation from Pb resulted in U concentrations of up to 6.83 ppm. Most of the garnets have low $^{206}Pb/^{204}Pb$ ratios < 150 and inter-element variations (Th/U, Sm/Nd, U/Nd) suggest that at least some of the U and Th is hosted in inclusions of monazite and zircon. A distinction whether monazite or zircon dominates the inclusion suite is important, because zircon is more likely than monazite to survive high-grade metamorphism and to induce a pre-metamorphic Pb signature upon the garnet. The range of trace element ratios for garnet, monazite and zircon results from combined effects of crystal structure and element availability during mineral growth. Variation in Sm/Nd may be primarily controlled by the size of the cation site into which Sm/Nd substitute since Sm/Nd in crustal rocks vary only very little. On the other hand, Th/U may vary significantly due to the stability of U^{6+}, which has no Th analog. Based on the results of previous studies (DeWolf et al.1996) we adopt Th/U > 3 for

monazite and allanite but Th/U $\ll 1$ for zircon. U/Nd in monazite may be low compared to zircon and garnet due to the high concentrations of Nd in monazite. This study has also shown that analysing garnets from different settings with different methods together with an evaluation of element ratios provides criteria for evaluating the role of submicroscopic inclusions and place constraints on the U and radiogenic Pb budgets of such garnets. The application of these techniques are essential in extracting meaningful ages from major rock forming minerals with low μ values such as garnet. Results obtained with these methods can be used to unravel P–T-t paths in high-grade metamorphic belts and help to better understand tectonometamorphic processes in high-grade terranes.

Acknowledgements This work was supported by the Max-Planck Society. S.J. would like to thank A.W. Hofmann for free access to lab and mass spectrometry facilities over the years. Discussions with W. Todt, U. Poller and A. Möller are highly appreciated. Iris Bambach is warmly thanked for her patient help with the figures. We gratefully acknowledge the very constructive and unbiased reviews given by B. Bingen and R. Frei, which helped to improve the original manuscript.

References

Bingen B, van Breemen O (1998) U-Pb monazite ages in amphibolite- to granulite-facies orthogneiss reflect hydrous mineral breakdown reactions: Sveconorwegian Province of SW Norway. Contrib Mineral Petrol 132:336–353

Bingen B, Demaiffe D, Hertogen D (1996) Redistribution of rare-earth elements, Th and U over accessory minerals in the course of amphibolite to granulite facies metamorphism: the role of apatite and monazite in orthogneisses from SW Norway. Geochim Cosmochim Acta 60:1341–1354

Braun I, Montel J-M, Nicollet C (1998) Electron microprobe dating of monazites from high-grade gneisses and pegmatites of the Kerala Khondalite Belt, southern India. Chem Geol 146:65–85

Briqueu L, Lancelot JR, Valois J-P, Walgenwitz F (1980) Géochronologie U-Pb et genèse d'un type de minéralisation uranifère: Les alaskites de Goanikontes (Namibie) et leur encaissant. Bull Cent Rech Expl-Prod Elf-Aquit 4:759–811

Burton KW, ÓNions RK (1991) High-resolution garnet chronometry and the rates of metamorphic processes. Earth Planet Sci Lett 107:649–671

Cameron AE, Smith DH, Walker RL (1969) Mass spectrometry of nanogram-size samples of lead. Anal Chem 41:525–526

Christensen JN, Rosenfeld JL, DePaolo DJ (1989) Rates of tectonometamorphic processes from rubidium and strontium isotopes in garnet. Science 244:1465–1469

Clemens JD, Wall VJ (1988) Controls on the mineralogy of S-type volcanic and plutonic rocks. Lithos 21:53–66

Cohen AS, ÓNions RK, Siegenthaler R, Griffin WL (1988) Chronology of the pressure-temperature history recorded by a granulite terrain. Contrib Mineral Petrol 98:303–311

Copeland P, Parrish RR, Harrison TM (1988) Identification of inherited radiogenic Pb in monazite and implications for U-Pb systematics. Nature 333:760–763

DeWolf CP, Belshaw NS, ÓNions RK (1993) A metamorphic history from micron-scale chronometry of monazite. Earth Planet Sci Lett 120:207–220

DeWolf CP, Zeissler CJ, Halliday AN, Mezger K, Essene EJ (1996) The role of inclusions in U-Pb and Sm-Nd garnet geochronology: Stepwise dissolution experiments and trace uranium mapping by fission track analysis. Geochim Cosmochim Acta 60:121–134

Erambert M, Austhreim H (1993) The effect of fluid and deformation on zoning and inclusion patterns in poly-metamorphic garnets. Contrib Mineral Petrol 115:204–214

Foster G, Kinny P, Vance D, Prince C, Harris N (2000) The significance of monazite U-Th-Pb age data in metamorphic assemblages; a combined study of monazite and garnet chronometry. Earth Planet Sci Lett 181:327–340

Harris NBW, Gravestock P, Inger S (1992) Ion-microprobe determinations of trace-element concentrations in garnets from anatectic assemblages. Chem Geol 100:41–49

Hartmann O, Hoffer E, Haack U (1983) Regional metamorphism in the Damara orogen: Interaction of crustal motion and heat transfer. In: Miller R McG (ed) Evolution of the Damara orogen. Spec Publ Geol Soc S Afr 11:233–241

Hawkins DP, Bowring SA (1997) U-Pb systematics of monazite and xenotime: case studies from the Paleaoproterozoic of the Grand Canyon, Arizona. Contrib Mineral Petrol 127:87–103

Hawkins DP, Bowring, SA (1999) U-Pb monazite, xenotime and titanite geochronological constraints on the prograde to post-peak metamorphic thermal history of Paleoproterozoic migmatites from the Grand Canyon, Arizona. Contrib Mineral Petrol 134:150–169

Henson BJ, Zhou B (1995) Retention of isotopic memory in garnets partially broken down during an overprinting granulite-facies metamorphism: Implications for the Sm-Nd closure temperature. Geology 23:225–228

Hickmott DD, Shimizu N, Spear FS, Selverstone J (1987) Trace element zoning in a metamorphic garnet. Geology 15:573–576

Hoernes S, Hoffer E (1979) Equilibrium relations of prograde metamorphic mineral assemblages—a stable isotope study of rocks of the Damara orogen. Contrib Mineral Petrol 68:377–389

Housh T, Bowring SA (1991) Lead isotopic heterogeneities within alkali feldspars: implications for the determination of initial lead composition. Geochim Cosmochim Acta 55:2309–2316

Humphries FJ, Cliff RA (1982) Sm-Nd dating and cooling history of Scourian granulites, Sutherland. Nature 295:515–517

Jagoutz E (1988) Nd and Sr systematics in an eclogite xenolith from Tanzania: Evidence for frozen mineral equilibria in continental lithosphere. Geochim Cosmochim Acta 52:1285–1293

Jung S (2001) High-temperature, low/medium-pressure clockwise P-T paths and melting in the development of regional migmatites: The role of crustal thickening and repeated plutonism. Geol J 35:345–359

Jung S, Hoernes S, Masberg P, Hoffer E (1999) The petrogenesis of some migmatites and granites (central Damara Orogen, Namibia): Evidence for disequilibrium melting, wall rock contamination and crystal fractionation. J Petrol 40:1241–1269

Jung S, Hoernes S, Mezger K (2000a) Origin of some Pan-African syn-tectonic S-type and post-tectonic A-type granites (Namibia)—products of melting of crustal sources, fractional crystallization and wall rock entrainment. Lithos 50:259–287

Jung S, Hoernes S, Mezger K (2000b) Geochronology and petrology of stromatic and nebulitic migmatites from the Proterozoic Damara Belt—importance of episodic fluid-present disequilibrium melting and consequences for granite petrology. Lithos 51:153–179

Jung S, Mezger K (2001) Geochronology in migmatites—a Sm-Nd, U-Pb and Rb-Sr study from the Proterozoic Damara belt (Namibia) and implications for polyphase development of migmatites in high-grade terranes. J Metamorph Geol 19:77–97

Jung S, Mezger K (2003) Petrology of basement-dominated terranes: I. Regional metamorphic T-t path and geochronological constraints on Pan-African high-grade metamorphism (central Damara orogen, Namibia). Chem Geol 198:223–247

Jung S, Mezger K, Hoernes S (1998b) Geochemical and isotopic studies of syenites from the Proterozoic Damara belt (Namibia): Implications for the origin of syenites. Mineral Mag 62A:729–730

Jung S, Mezger K, Hoernes S (2001) Trace element and isotopic (Sr, Nd, Pb, O) arguments for a mid crustal origin of

Pan-African garnet-bearing S-type granites from the Damara orogen (Namibia). Precambrian Res 110:325–355
Jung S, Mezger K, Hoernes S (2003) Petrology of basement-dominated terranes: II. Contrasting isotopic (Sr, Nd, Pb and O) signatures of basement-derived granites and constraints on the source region of granite (Damara orogen, Namibia). Chem Geol 199:1-28 (in press)
Jung S, Mezger K, Masberg P, Hoffer E, Hoernes S (1998a) Petrology of an intrusion-related high-grade migmatite: implications for partial melting of metasedimentary rocks and leucosome-forming processes. J Metamorph Geol 16:425–445
Kingsbury JA, Miller CF, Wooden JL, Harrison MT (1993) Monazite paragenesis and U-Pb systematics in rocks of the eastern Mojave Desert, California, USA: implications for thermochronometry. Chem Geol 110:147–167
Kukla C, Kramm U, Kukla PA, Okrusch M (1991) U-Pb monazite data relating to metamorphism and granite intrusion in the northwestern Khomas Trough, Damara Orogen, central Namibia. Commun Geol Surv Namibia 7:49–54
Lanzirotti A, Hanson GN (1995) U-Pb dating of major and accessory minerals formed during metamorphism and deformation of metapelites. Geochim Cosmochim Acta 59:2513–2526
Lanzirotti A, Hanson GN (1996) Geochronology and geochemistry of multiple generations of monazite from the Wepawaug schists, Connecticut, USA: implications for monazite stability in metamorphic rocks. Contrib Mineral Petrol 125:332–340
Ludwig KR, Silver LT (1977) Lead isotope inhomogeneity in Precambrian igneous K-feldspars. Geochim Cosmochim Acta 41:1457–1471
Ludwig KR (1991a) PBDAT: a computer program for processing Pb-U-Th isotope data, Version 2.75. US Geol Surv Open File Rep 88–542
Ludwig KR (1991b) ISOPLOT: a plotting and regression program for radiogenic isotope data, Version 2.75. US Geol Surv Open File Rep 91–445
Maboko MAH, Nakamura E (1995) Sm-Nd garnet ages from the Uluguru granulite complex of Eastern Tanzania: further evidence for post-metamorphic slow cooling in the Mozambique belt. Precambrian Res 74:195–202
Masberg HP, Hoffer E, Hoernes S (1992) Microfabrics indicating granulite-facies metamorphism in the low-pressure central Damara Orogen, Namibia. Precambrian Res 55:243–257
Mattinson JM (1986) Geochronology of high-pressure-low temperature Franciscan metabasites. A new approach using the U-Pb system. Geol Soc Am Mem 164:95–105
Mezger K, Hanson GN, Bohlen SR (1989) U-Pb systematics of garnet: dating the growth of garnet in the Late Archean Pikwitonei granulite domain at Cauchon and Natawahunan Lakes, Manitoba, Canada. Contrib Mineral Petrol 101:136–148
Mezger K, Essene EJ, Halliday AN (1992) Closure temperature of the Sm-Nd system in metamorphic garnets. Earth Planet Sci Lett 113:397–409
Miller R McG (1983) The Pan-African Damara Orogen of South West Africa/Namibia. In: Miller R McG (ed) Evolution of the Damara orogen. Spec Publ Geol Soc S Afr 11:431–515
Möller A, Mezger K, Schenk V (2000) U-Pb dating of metamorphic minerals: Pan-African metamorphism and prolonged slow cooling of high-pressure granulites in Tanzania, East Africa. Precambrian Res 104:123–146
Moyes AB, Groenewald PB (1996) Isotopic constraints on Pan-African metamorphism in Dronning Maud Land, Antartica. Chem Geol 129:247–256
Mork MBE, Means EW (1986) Sm-Nd systematics of a gabbro-eclogite transition. Lithos 19:255–267
Paterson BA, Rogers G, Stevens WE (1992) Evidence for inherited Sm-Nd isotopes in granitoid zircon. Contrib Mineral Petrol 111:378–390
Parrish RR (1990) U-Pb dating of monazite and its application to geological problems. Can J Earth Sci 27:1435–1450
Parrish RR, Tirull R (1989) U-Pb age of the Baltoro granite, northwest Himalaya, and implications for monazite systematics. Geology 17:1076–1079
Poller U, Huth J, Hoppe P, Williams IS (2001) REE, U, Th, and Hf distribution in zircon from western Carpathian variscan granitoids: a combined cathodoluminescence and ion microprobe study. Am J Sci 301:858–876
Prince CI, Kosler J, Vance D, Günther D (2000) Comparison of laser ablation ICP-MS and isotope dilution REE analyses—implications for Sm-Nd garnet geochronology. Chem Geol 168:255–274
Puhan D (1983) Temperature and pressure of metamorphism in the Central Damara orogen. In: Miller R McG (ed) Evolution of the Damara orogen. Spec Pub Geol Soc S Afr 11:219–223
Schärer U (1984) The effect of initial ^{230}Th disequilibrium on young U-Pb ages: The Makalu case, Himalaya. Earth Planet Sci Lett 67:191–204
Schmidt A, Wedepohl KH (1983) Chemical composition and genetic relations of the Matchless amphibolite (Damara orogenic belt). Spec Publ Geol Soc S Afr 11:139–145
Sevigny JH (1993) Monazite controlled Sm/Nd fractionation in leucogranites: an ion microprobe study of garnet phenocrysts. Geochim Cosmochim Acta 57:4095–4102
Smith HA, Barreiro BA (1990) Monazite U-Pb dating of staurolite grade metamorphism in pelitic schists. Contrib Mineral Petrol 105:602–615
Stowell HH, Goldberg SA (1997) Sm-Nd garnet dating of polyphase metamorphism: northern Coast Mountains, south-east Alaska, USA. J Metamorph Geol 15:439–450
Suzuki K, Adachi M, Kajizuka I (1994) Electron microprobe observations of Pb diffusion in metamorphosed detrital monazites. Earth Planet Sci Lett 128:391–405
Vance D, O'Nions RK (1990) Isotopic chronometry of zoned garnets: Growth kinetics and metamorphic histories. Earth Planet Sci Lett 97:227–240
Vance D, Harris N (1999) Timing of prograde metamorphism in the Zanskar Himalaya. Geology 27:395–398
Vance D, Meier M, Oberli F (1998) The influence of high U-Th inclusions on the U-Th-Pb systematics of almandine-pyrope garnet: results of a combined bulk dissolution, stepwise-leaching, and SEM study. Geochim Cosmochim Acta 62:3527–3540
Vance D, Strachan RA, Jones KA (1998) Extensional versus compressional setting for metamorphism: Garnet chronometry and pressure-temperature-time histories in the Moine Supergroup, northwest Scotland. Geology 26:927–930
von Blanckenburg F (1993) Combined high-precision chronometry and geochemical tracing using accessory minerals applied to the Central-Alpine Bergell intrusion (central Europe). Chem Geol 100:19–40
von Quadt A (1992) U-Pb zircon and Sm-Nd geochronology of mafic and ultramafic rocks from the central part of the Tauern window (eastern Alps). Contrib Mineral Petrol 110:57–67
Zhou B, Henson BJ (1995) Inherited Sm/Nd isotope components preserved in monazite inclusions within garnets in leucogneiss from East Antarctica and implications for closure temperature studies. Chem Geol 121:317–326